Article

Dynamics of Epidemic Spreading in the Group-Based Multilayer Networks

Dong Wang, Yi Zhao * and Hui Leng

School of Science, Harbin Institute of Technology (Shenzhen), Shenzhen 518055, China;
dong.wang@stu.hit.edu.cn (D.W.); hui_leng@163.com (H.L.)
* Correspondence: zhao.yi@hit.edu.cn

Abstract: The co-evolution between information and epidemic in multilayer networks has attracted wide attention. However, previous studies usually assume that two networks with the same individuals are coupled into a multiplex network, ignoring the context that the individuals of each layer in the multilayer network are often different, especially in group structures with rich collective phenomena. In this paper, based on the scenario of group-based multilayer networks, we investigate the coupled UAU-SIS (Unaware-Aware-Unaware-Susceptible-Infected-Susceptible) model via microscopic Markov chain approach (MMCA). Importantly, the evolution of such transmission process with respective to various impact factors, especially for the group features, is captured by simulations. We further obtain the theoretical threshold for the onset of epidemic outbreaks and analyze its characteristics through numerical simulations. It is concluded that the growth of the group size of information (physical) layer effectively suppresses (enhances) epidemic spreading. Moreover, taking the context of epidemic immunization into account, we find that the propagation capacity and robustness of this type of network are greater than the conventional multiplex network.

Keywords: spreading dynamics; group-based networks; MMCA; collective phenomenon; robustness

1. Introduction

Recently, spreading dynamics has attracted a lot of attention in the field of complex networks [1–4], and plenty of studies have been devoted to investigate epidemic spreading [5,6], information diffusion [7,8], rumor dissemination [9,10], and credit contagion [11]. Two classical mathematical frameworks, i.e., SIS model [1] and SIR model [12], are widely used to study spreading processes. The previous works in the literature are mainly based on single-layer networks. However, in reality, single-layer networks do not exist alone, but usually interplay together and couple into multilayer networks [13–15]. For example, one can place physical contacts with family, friends, and colleagues in one layer, and place virtual contacts (e.g., online social networks) in another. The spreading dynamics in multilayer networks and that in single-layer networks can be fundamentally different [16–19].

As a consequence, researchers increasingly concentrate on multilayer networks to study the epidemic spreading. Granell et al. [18] first propose a UAU-SIS model, where the microscopic Markov chain approach (MMCA) [20] is used for describing the coupled transmission process between information diffusion in virtual layer (UAU) and epidemic spreading in physical layer (SIS). They thus investigate the effect of mass media on the propagation process [19]. Along this line, other studies extend the co-evolution model by considering more influencing factors [21,22]. Moreover, more effects are further investigated, such as nonlinear coupled multiplex networks [23], resource control [24], global awareness [25], awareness cascade [26], time varying transmission rates [27,28], epidemic suppression [29,30] and coupled spreading process based on SIR model [31,32].

Please note that the studies above are primarily based on multiplex networks [33–35], in which each node in one layer has its unique counterpart in another layer.

However, the multiplex network may not tell the whole story of multilayer networks. In reality, there exist many multilayer networks that different layers are coupled by different entities [36]. In addition, there are some diseases (e.g., hand-foot-and-mouth epidemic) that spread only among children, and adults (e.g., children's parents) can exchange the information about epidemics. The adults who have known the epidemic information can take measures to protect their children, thereby inhibiting the spread of the disease. At the same time, infected children will let the adults know the information about the epidemic, thereby promoting the diffusion of epidemic information. So the interactive adults and children are coupled together to form a bilayer network: adult layer for information diffusion is regarded as the information layer and children's layer for epidemic spreading is regarded as physical layer. Naturally, internal family members have rich collective phenomena and are closely linked, while the connections between families are usually sparse. As a result, the nodes of the bilayer network can be divided into many groups, and we call the network as the group-based bilayer network. Nevertheless, such type of multilayer network has seldom been studied.

In this paper, we focus on the dynamics of epidemic spreading by considering the proposed group-based bilayer networks (see the details in Section 2.1). Distinct from previous works, we assume that the nodes of a group in information layer first reach consensus and then act on the corresponding nodes in physical layer through the inter-layer feedback mechanism. Inspired by the works in [18,19], we further reveal the epidemic propagation dynamics over such type of networks and explicitly derive the meta-critical point of epidemic spreading outbreaks based on MMCA. Moreover, we study the variations of epidemic spreading under both random and deliberate network attacking strategies, thereby giving the relationship between the propagation capability and the corresponding network topology.

The paper is organized as follows. In Section 2, the UAU-SIS model for the coupled group-based multilayer networks is described in detail. In Section 3, we employ MMCA to analyze the dynamical propagation process based on the previous model, and conduct numerical simulations to investigate the effects of different parameters. Then the theoretical discussion of the propagation threshold is given in Section 4. In particular, we study the robustness of network propagation in Section 5. Finally, we take the conclusion in Section 6.

2. Model

2.1. Structural Representation of Group-Based Multilayer Networks

A coupled UAU-SIS dynamics is modeled based on the group-based multilayer network, as illustrated in Figure 1. We first introduce the method of constructing the group-based multilayer networks. The sequence $\{x_i\}_{i=1}^n$ stands for the set of group sizes in the information layer, where n is the number of groups. The intra-group members are fully connected and we use $X = \{x_{ij}\}_{i,j=1}^M$ ($x_{ij} = 1$ if two nodes i and j of the information layer are in the same group, $x_{ij} = 0$ otherwise) to represent the corresponding adjacent matrix. The inter-group members are randomly connected based on Erdös-Rényi network [37], denoted as $G(M, p)$, where $M = \sum_{i=1}^n x_i$ denotes the number of nodes of information layer, and p is the random connection probability. Then we use $\mathscr{A} = \{a_{ij}\}_{i,j=1}^M [= X \cup G(M, p)]$ to represent the whole adjacent matrix of information layer. Similarly, the sequence $\{y_j\}_{j=1}^n$ describes the set of group size in the physical layer, where intra-group individuals are fully connected and the inter-group individuals are also randomly linked according to Erdös-Rényi network $G(N, p)$ with $N = \sum_{i=1}^n y_i$ the number of nodes of physical layer and p the random connection probability. Please note that both layers have the same number of groups, each of which has its corresponding counterpart in another layer. Analogously, the matrices $Y = \{y_{ij}\}_{i,j=1}^N$ ($y_{ij} = 1$ if two nodes i and j of the physical layer are in the same group, $y_{ij} = 0$ otherwise) and $\mathscr{B} = \{b_{ij}\}_{i,j=1}^N [= Y \cup G(N, p)]$ represent the intra-group and the whole adjacent matrices of physical

layer, respectively. Finally, $\mathscr{C} = \{c_{ij}\}$ ($i = 1, \ldots, N$, $j = 1, \ldots, M$) is used to describe the inter-layer relationship. If the node i of the physical layer is in the same group as the node j of the information layer, $c_{ij} = 1$; otherwise, $c_{ij} = 0$. We assume that if there is a link between the physical layer groups, there is at least one link between the corresponding groups of the information layer. The obtained group-based multilayer network has strong homogeneity, i.e., intra-group homogeneity (i.e., the nodes within the group are fully connected) and inter-group homogeneity (i.e., inter-groups are linked based on the Erdös-Rényi random network which is a typical homogeneous network). For convenience of reading, we summarize the key parameters in Table 1.
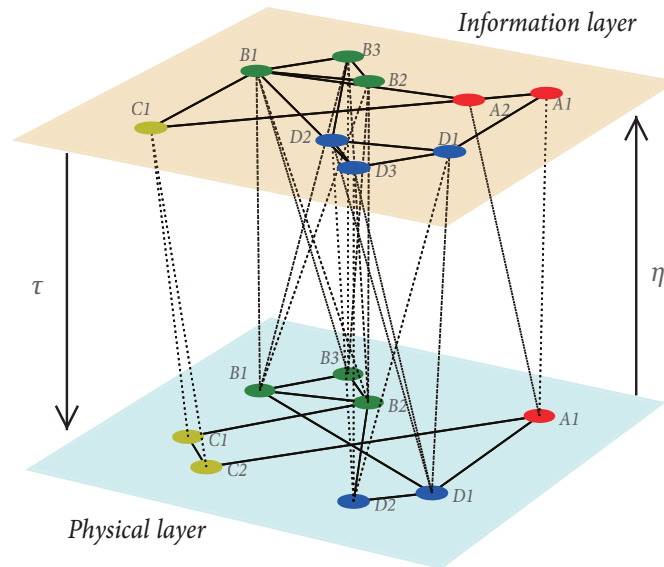

Figure 1. Schematic diagram of a coupled group-based bilayer network. The upper (lower) layer stands for the information diffusion (epidemic spreading), where each node in the information (physical) layer only has two possible states: aware (A) and unaware (U) [susceptible (S) and infected (I)]. τ (η) represents the feedback intensity from information (physical) layer to physical (information) layer. The nodes in the same color belong to the same group in each layer.

Table 1. The description of the related key parameters.

Parameter	Description
τ	Feedback intensity from information layer to physical layer
η	Feedback intensity from physical layer to information layer
x_i	Group size of information layer where node i belongs
y_i	Group size of physical layer where node i belongs
X	Group-matrix of information layer
Y	Group-matrix of physical layer
β_1^U	Infection probability for intra-group unsuppressed nodes
β_2^U	Infection probability for inter-group unsuppressed nodes
β_1^A	Infection probability for intra-group suppressed nodes
β_2^A	Infection probability for inter-group suppressed nodes
λ_1	Information diffusion probability of intra-group
λ_2	Information diffusion probability of inter-group
γ	Attenuation factor
ρ	The density of infected individuals
μ	Probability of recovery
δ	Probability of forgetting
ι	Proportion of intra-group and inter-group transmission

2.2. Coupled Spreading Processes

The coupled propagation dynamics involves two processes: SIS in the physical layer and UAU in the information layer. In the physical layer, the nodes are susceptible (S) or infected (I); and in the information layer, the nodes are aware (A) or unaware (U). Assuming that the nodes of the information layer and the nodes of the physical layer are in the same group, we describe the epidemic spreading process. If the information layer nodes are unaware, then the susceptible nodes will be infected by the normal probabilities β_1^U (when it contacts an intra-group infected node) and β_2^U (when it contacts an inter-group infected node). If the information layer nodes are aware, the susceptible nodes have a chance of being infected by a lower probability, i.e., $\beta_1^A = \gamma\beta_1^U$ for intra-group contacts and $\beta_2^A = \gamma\beta_2^U$ for inter-group contacts, where γ is the attenuation factor ranging from 0 to 1. We note that unlike the multiplex network, since two layer agents of this type of multilayer network are different, the awareness of the information layer nodes does not mean that the physical layer nodes are alerted. We define a ratio $\iota = \frac{\beta_1^U}{\beta_2^U} = \frac{\beta_1^A}{\beta_2^A}$ that is used to distinguish the propagation of intra-group and inter-group, where $\iota > 1$ denotes that the transmission in intra-group is faster than that in inter-group. Assume that each I-state node has a probability of spontaneous recovery μ, which is unrelated to whether it is alerted.

The information diffusion in the information layer motivates people to take measures to suppress the epidemic spreading through inter-layer connections. The agents of a group in information layer first reach consensus and then provide feedback to the corresponding agents within the same group in the physical layer through the feedback intensity $f^{X \to Y}$ which is described in Equation (2). As for the process of information diffusion, the U-state nodes in the information layer can be perceived by intra-group nodes (with diffusion probability λ_1), inter-group nodes (with diffusion probability λ_2) and infected nodes which belong to the same group (with feedback intensity η) in the physical layer. Meanwhile, an A-state node could then turn into unaware with the forgetting probability δ. We note that the two inter-layer feedback mechanisms are different, i.e., for the feedback from information layer to physical layer, the nodes of information layer first reach consensus and then perform a feedback by the whole group intensity $f^{X \to Y}$; for the feedback from physical layer to information layer, the I-state individual acts on the corresponding group of information layer via the feedback intensity η directly.

3. Microscopic Markov Chain Approach

3.1. Theoretical Analysis

In this section, we conduct a theoretical analysis of the above model by resorting to MMCA. Initially, a node i in the physical layer together with its counterpart nodes in the information layer has four possible coupled states in a probabilistic sense: AI (aware and infected), AS (aware and susceptible), UI (unaware and infected), and US (unaware and susceptible). For node i of the physical layer, we assume that all nodes in the same group of the information layer are j ($j = 1, \cdots, x_i$), and then define the group consensus of these nodes by the average awareness probability, i.e., $p_i^A(t) = \frac{1}{x_i}\sum_{j=1}^{x_i} p_{ij}^A(t)$. Moreover, these probabilities satisfy the normalization condition

$$p_i^{AI}(t) + p_i^{AS}(t) + p_i^{UI}(t) + p_i^{US}(t) = 1. \tag{1}$$

Here we focus on the propagation dynamics of epidemic spreading which is influenced by the process of information diffusion. For the sake of brevity, we just give discrete transition probability tress for the nodes of physical layer in Figure 2, where $A_A S$ ($A_U S$) denotes that the S-state nodes have (not) been alerted by A-state nodes, thereby getting infected with the small (normal) probability, i.e., β_1^A (β_1^U) for intra-group propagation and β_2^A (β_2^U) for inter-group propagation. We note that in the transition probability trees in Figure 2a,b, the state changes of the I-state node are unrelated to whether it is alerted or not, so we do not need to distinguish the states $A_A I$ and $A_U I$ and merely use AI.

Considering the impact of group structure, we update the feedback intensity from the information layer to the physical layer by

$$f_i^{X \to Y} = 1 - (1 - \tau)^{x_i}, \tag{2}$$

which inhibits the infection of the S-state node i with lower infection probability. Apparently, $f_i^{X \to Y}$ degenerates into τ when the group size $x_i = 1$.
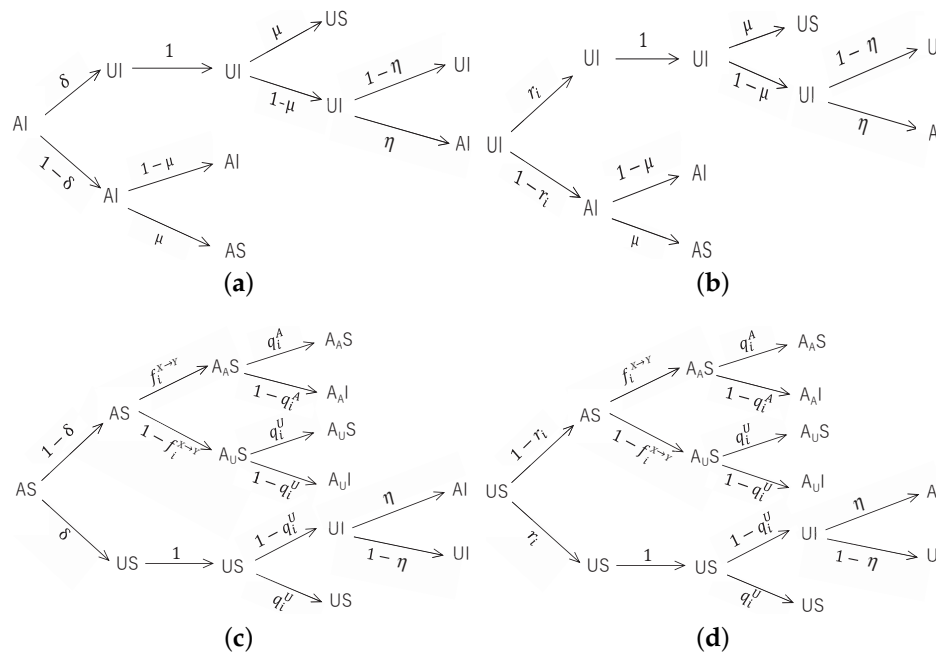

Figure 2. Transition probability trees for the states (**a**) AI, (**b**) UI, (**c**) AS, (**d**) US. Each tree includes four stages: information diffusion (UAU process), feedback from the information layer to the physical layer, epidemic spreading (SIS process), and feedback from the physical layer to the information layer.

We use $r_{ij}(t)$ to denote the probability that the unaware node j does not enter into the aware state (node j of information layer and node i of physical layer are in the same group),

$$r_{ij}(t) = c_{ij} \prod_{k \in X_j} [1 - a_{jk} p_k^A(t) \lambda_1] \times \prod_{k \notin X_j} [1 - a_{jk} p_k^A(t) \lambda_2]. \tag{3}$$

Equation (3) can also be written as $r_{ij}(t) = c_{ij} \prod_k [1 - x_{jk} p_k^A(t) \lambda_1] \times \prod_k [1 - (a_{jk} - x_{jk}) p_k^A(t) \lambda_2]$, where $p_k^A(t) = p_k^{AI}(t) + p_k^{AS}(t)$. Based on the homogeneity of the network, for a given node i of the physical layer, we use $r_i(t) = \frac{1}{x_i} \sum_{j=1}^{x_i} r_{ij}(t)$ to denote the probability that its information layer nodes are not perceived.

Let $q_i^A(t)$ and $q_i^U(t)$ be the probability of node i not being infected by any neighbors if node i has and has not suppressed by the information layer, respectively. They are defined as:

$$q_i^A(t) = \prod_{j \in Y_i} [1 - b_{ji} p_j^I(t) \beta_1^A] \times \prod_{j \notin Y_i} [1 - b_{ji} p_j^I(t) \beta_2^A], \tag{4}$$

$$q_i^U(t) = \prod_{j \in Y_i} [1 - b_{ji} p_j^I(t) \beta_1^U] \times \prod_{j \notin Y_i} [1 - b_{ji} p_j^I(t) \beta_2^U]. \tag{5}$$

Analogously, both equations can also be read as $q_i^A(t) = \prod_j [1 - y_{ji} p_j^I(t) \beta_1^A] \times \prod_j [1 - (b_{ji} - y_{ji}) p_j^I(t) \beta_2^A]$, and $q_i^U(t) = \prod_j [1 - y_{ji} p_j^I(t) \beta_1^U] \times \prod_j [1 - (b_{ji} - y_{ji}) p_j^I(t) \beta_2^U]$, respectively.

According to the state transition trees in Figure 2, we obtain the dynamical equations of the whole model as follows:

$$p_i^{US}(t+1) = p_i^{AI}(t)\delta\mu + p_i^{AS}(t)\delta q_i^{U}(t) + p_i^{UI}(t)r_i(t)\mu + p_i^{US}(t)r_i(t)q_i^{U}(t), \tag{6}$$

$$\begin{aligned}
p_i^{UI}(t+1) = {} & p_i^{AI}(t)\delta(1-\mu)(1-\eta) + p_i^{AS}(t)\delta[1 - q_i^{U}(t)](1-\eta) \\
& + p_i^{UI}(t)r_i(t)(1-\mu)(1-\eta) + p_i^{US}(t)r_i(t)[1 - q_i^{U}(t)](1-\eta),
\end{aligned} \tag{7}$$

$$\begin{aligned}
p_i^{AS}(t+1) = {} & p_i^{AI}(t)(1-\delta)\mu + p_i^{AS}(t)(1-\delta)\{(1 - f_i^{X\to Y})q_i^{U}(t) + f_i^{X\to Y}q_i^{A}(t)\} \\
& + p_i^{UI}(t)[1 - r_i(t)]\mu + p_i^{US}[1 - r_i(t)]\{(1 - f_i^{X\to Y})q_i^{U}(t) + f_i^{X\to Y}q_i^{A}(t)\},
\end{aligned} \tag{8}$$

$$\begin{aligned}
p_i^{AI}(t+1) = {} & p_i^{AI}(t)[\delta(1-\mu)\eta + (1-\delta)(1-\mu)] \\
& + p_i^{AS}(t)\{\delta[1 - q_i^{U}(t)]\eta + (1-\delta)[(1 - q_i^{U}(t))(1 - f_i^{X\to Y}) + (1 - q_i^{A}(t))f_i^{X\to Y}]\} \\
& + p_i^{UI}\{r_i(t)(1-\mu)\eta + [1 - r_i(t)](1-\mu)\} \\
& + p_i^{US}(t)\{[1 - r_i(t)][(1 - f_i^{X\to Y})(1 - q_i^{U}(t)) + f_i^{X\to Y}(1 - q_i^{A}(t))] + r_i(t)[1 - q_i^{U}(t)]\eta\}.
\end{aligned} \tag{9}$$

Then combining Equations (1)–(9), we can simulate the evolution process of the epidemic spreading coupled by information diffusion for any initial state, and then can iteratively solve the expected infection density $\rho = \frac{1}{N}\sum_{i=1}^{N} p_i^{I} = \frac{1}{N}\sum_{i=1}^{N}(p_i^{UI} + p_i^{AI})$ in steady state, where p_i^{I} denotes the infected possibility of node i of physical layer.

3.2. Numerical Simulations

In this section, we investigate the influence of several critical parameters on the spreading prevalence of such propagation system. We construct the group-based multilayer networks based on the method described in Section 2.1. Here, a sequence $\{x_i\}_{i=1}^{n}$ that obeys a uniform distribution $U(1, 2 \cdot \bar{x} - 1)$ is used to determine the group sizes of the information layer, where $\bar{x}$ is the mean value of the group sizes. Similarly, we can get the sequence $\{y_i\}_{i=1}^{n}$ of the group sizes of the physical layer under $U(1, 2 \cdot \bar{y} - 1)$, where $\bar{y}$ is the mean value. We note that the group-based multilayer network degenerates into the multiplex network when the group sizes $\bar{x}$ and $\bar{y}$ are set to 1. As a comparison with MMCA, Monte Carlo (MC) simulations are also presented. We initially set $p_i^{I} = p_i^{A} = 0.1$ for each node. Figure 3a,b show the spreading prevalence ρ as functions of $\beta(= \beta_2^{U})$ for different attenuation factor γ and recovery probability μ, respectively.

It is obvious that the density of I-state nodes ρ is positively correlated with the propagation probability β (i.e., ρ increases with the growth of β). Epidemic cannot spread when the propagation probability β is smaller than specific values that are defined as the threshold of spreading processes. We notice that the threshold declines as the attenuation factor γ increases, thereby implying that the epidemic is easier to break out with a lower level of suppression. Accordingly, the infection density ρ increases with the growth of γ. Figure 3b clearly shows that the increase of μ reduces ρ, which indicates that the recovery probability μ plays a vital role in spreading dynamics. As shown in Figure 3, the accordance trend is basically consistent between MC and MMCA.

In addition, we focus on the epidemic spreading prevalence with respective to the mean group size of information (physical) layer $\bar{x}$ ($\bar{y}$) so as to observe the relationship between ρ and $\bar{x}$, $\bar{y}$ with statistical significance.

Figure 4a shows that the increasing average group size of the information layer $\bar{x}$ leads to the decrease of ρ. It is reasonable that the larger group size of the information layer brings about stronger suppression from information layer to physical layer. Concerning the group size of the physical layer $\bar{y}$, in Figure 4b, the infection density ρ exhibits a significant increasing trend with the increase of $\bar{y}$. The group size growth of physical layer is inclined to promote epidemic spreading within the group, which consequently enhances the spreading prevalence.

In Figure 5, we show the I-state density ρ over the associated combinations of $\beta - \tau$ and $\beta - \lambda$. In the context of a small infection probability β, the I-state density ρ is approximately independent of the parameter τ because the spread cannot breakout, as shown in Figure 5a. It is natural that ρ decreases when the feedback parameter from information layer to physical layer τ increases in the case of big β. From Figure 5b, we find that the enhancement of information diffusion (caused by the increase of information diffusion probability λ) inhibits epidemic spreading. The full phase diagrams show a good agreement for ρ derived by MMCA and MC, hence we can use MMCA to approximate the group-based multilayer dynamics.
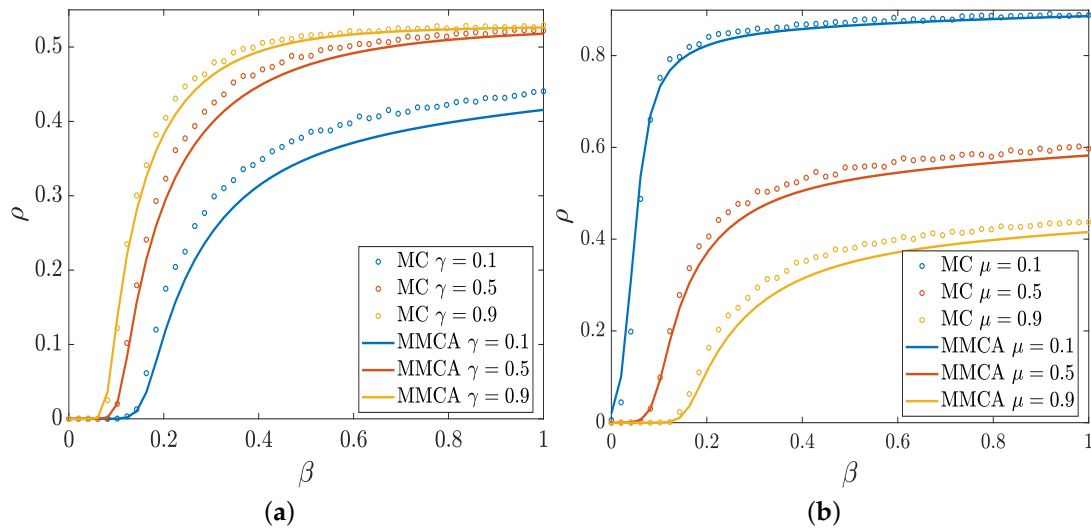
Figure 3. The infection density ρ as a function of the infectivity parameter β for different values of γ (**a**) and different values of μ (**b**). The result of (**a**) is obtained for $\mu = 0.9$ and that of (**b**) is for $\gamma = 0.1$. And the other parameter values are set to $\lambda_1 = \eta = 0.9$, $\lambda_2 = \tau = \delta = 0.5$, $\iota = 1.1$, $\bar{x} = \bar{y} = 3$.
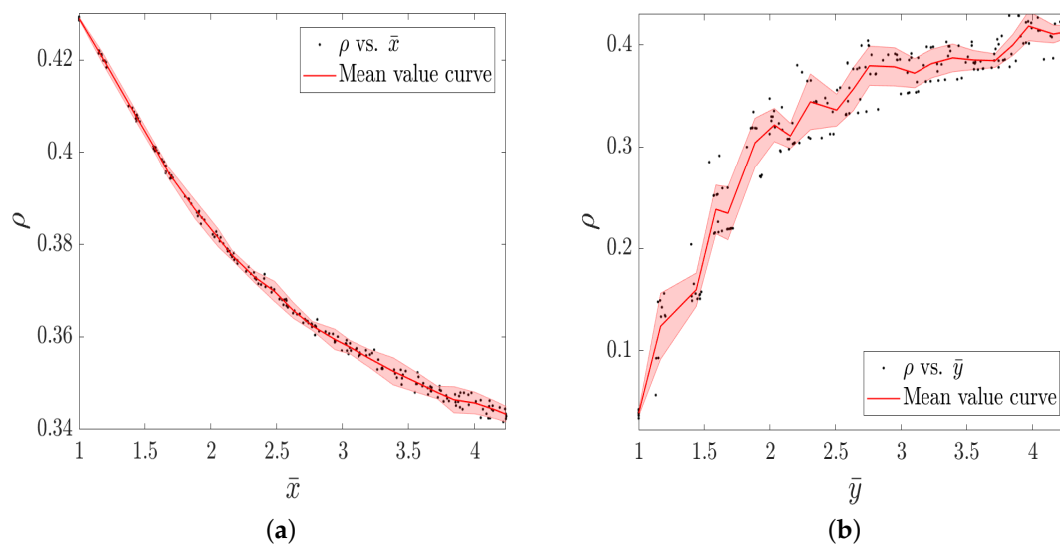

Figure 4. The infection density ρ as a function of the mean group size of information layer $\bar{x}$ (**a**) and physical layer $\bar{y}$ (**b**), respectively. The rest of other parameter values are fixed as: $\gamma = 0.1$, $\beta = \tau = \delta = \lambda_2 = 0.5$, $\iota = 1.1$, $\lambda_1 = \eta = \mu = 0.9$. When studying the effect of $\bar{x}$ ($\bar{y}$) on the spreading prevalence, we set $\bar{y} = 3$ ($\bar{x} = 3$).
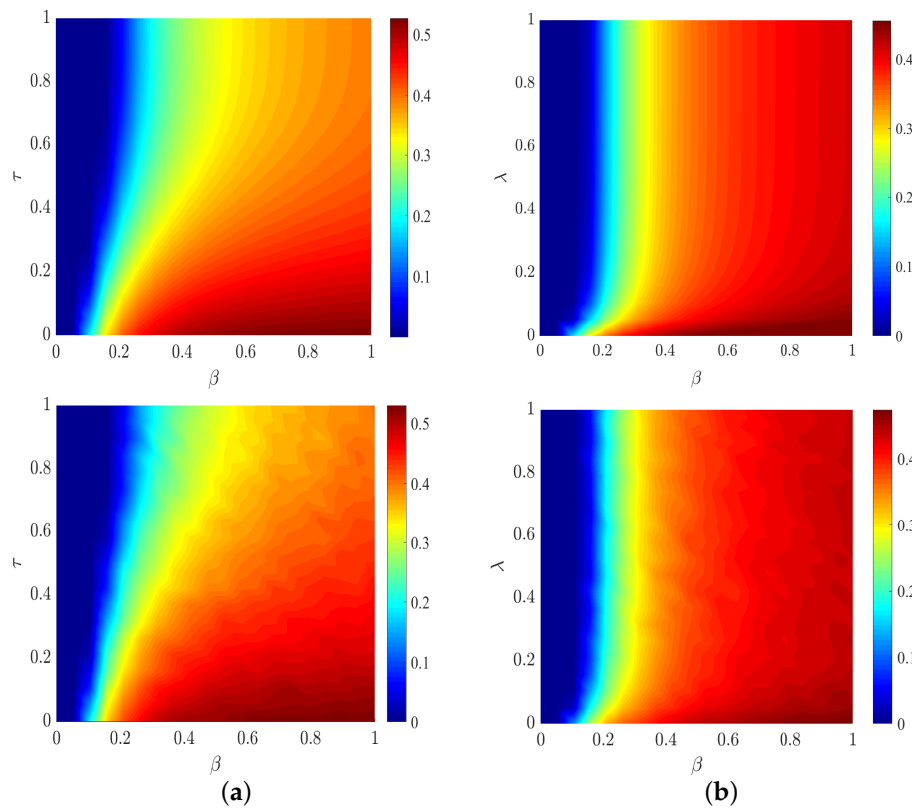
Figure 5. Phase diagrams of the group-based coupled propagation processes on the plane of $\beta - \tau$ (**a**) and $\beta - \lambda$ (**b**), where the results in the top panels are obtained by MMCA and those in the bottom panels are obtained by MC. For (**a**), other parameters are set to $\gamma = 0.1$, $\mu = \lambda_1 = \eta = 0.9$, $\iota = 1.1$, $\beta = \delta = \lambda_2 = 0.5$, $\bar{x} = \bar{y} = 3$. For (**b**), the parameter values are $\tau = 0.5$, $\lambda = \lambda_1 = \lambda_2$, and others are the same as those of (**a**).

4. The Outbreak Threshold of Epidemic Spreading

4.1. Theoretical Discussion

Next, we investigate the meta-critical point of the epidemic spreading. Combing Equations (7) and (9), the density of I-state nodes can be rewritten as

$$
\begin{aligned}
p_i^I = {} & p_i^I(1-\mu) + p_i^I(1-\mu) + p_i^{AS}\{\delta(1-q_i^U) + (1-\delta)[(1-q_i^U)(1-f_i^{X\to Y}) + (1-q_i^A)f_i^{X\to Y}]\} \\
& + p_i^{US}\{r_i(1-q_i^U) + (1-r_i)[(1-q_i^U)(1-f_i^{X\to Y}) + (1-q_i^A)f_i^{X\to Y}]\}.
\end{aligned}
\tag{10}
$$

Assuming that around the onset of the epidemic, the probability of I-state nodes is close to zero i.e., $p_i^I = \epsilon_i \ll 1$, Equations (4) and (5) are approximated by

$$
q_i^U \approx 1 - \beta_1^U \sum_j y_{ji}\epsilon_j - \beta_2^U \sum_j (b_{ji} - y_{ji})\epsilon_j = 1 - \beta_2^U \sum_{j=1}^N [b_{ji} + (\iota - 1)y_{ji}]\epsilon_j = 1 - \sigma_i,
\tag{11}
$$

$$
q_i^A \approx 1 - \gamma\beta_1^U \sum_j y_{ji}\epsilon_j - \gamma\beta_2^U \sum_j (b_{ji} - y_{ji})\epsilon_j = 1 - \gamma\beta_2^U \sum_{j=1}^N [b_{ji} + (\iota - 1)y_{ji}]\epsilon_j = 1 - \gamma\sigma_i,
\tag{12}
$$

where $\sigma_i = \beta_2^U \sum_{j=1}^N [b_{ji} + (\iota - 1)y_{ji}]\epsilon_j$.

Then Equation (10) is given by

$$
\begin{aligned}
\epsilon_i =& \epsilon_i(1-\mu) + p_i^{AS}\{\delta\sigma_i + (1-\delta)[\sigma_i(1-f_i^{X\to Y}) + \gamma\sigma_i f_i^{X\to Y}]\} \\
&+ p_i^{US}\{r_i\sigma_i + (1-r_i)[\sigma_i(1-f_i^{X\to Y}) + \gamma\sigma_i f_i^{X\to Y}]\} \\
=& \epsilon_i(1-\mu) + \gamma\sigma_i\{p_i^{AS}f_i^{X\to Y}(1-\delta) + p_i^{US}(1-r_i)f_i^{X\to Y}\} \\
&+ \sigma_i\{p_i^{AS}[\delta + (1-\tau)^{x_i}(1-\delta)] + p_i^{US}[r_i + (1-r_i)(1-\tau)^{x_i}]\} \\
=& \epsilon_i(1-\mu) + \gamma\sigma_i f_i^{X\to Y}\{p_i^{AS}(1-\delta) + p_i^{US}(1-r_i)\} \\
&+ \sigma_i\{p_i^{AS}\delta + p_i^{US}r_i + (1-f_i^{X\to Y})[p_i^{AS}(1-\delta) + p_i^{US}(1-r_i)]\}.
\end{aligned}
\tag{13}
$$

In the similar way, we can get

$$
\begin{aligned}
p_i^A &= p_i^{AS} + p_i^{AI} \approx p_i^A(1-\delta) + p_i^U(1-r_i), \\
p_i^U &= p_i^{US} + p_i^{AS} \approx p_i^A\delta + p_i^U r_i.
\end{aligned}
\tag{14}
$$

Substituting Equation (14) in Equation (13) leads to

$$
\begin{aligned}
\mu\epsilon_i &= \sigma_i\{\gamma f_i^{X\to Y}p_i^A + p_i^U + (1-f_i^{X\to Y})p_i^A\} \\
&= \beta_2^U\sum_{j=1}^N [b_{ji} + (\iota-1)y_{ji}]\epsilon_j[1-(1-\gamma)f_i^{X\to Y}p_i^A] \\
&= \beta_2^U\sum_{j=1}^N [b_{ji} + (\iota-1)y_{ji}][1-(1-\gamma)f_i^{X\to Y}p_i^A]\epsilon_j.
\end{aligned}
\tag{15}
$$

The above formula can be rewritten as

$$
\sum_{j=1}^N \{[1-(1-\gamma)f_i^{X\to Y}p_i^A][b_{ji} + (\iota-1)y_{ji}] - \frac{\mu}{\beta_2^U}\delta_{ji}\}\epsilon_j = 0,
\tag{16}
$$

where δ_{ji} is the element of the identity matrix.

We aim to determine the outbreak threshold of epidemic spreading process, so the lowest critical value β is given by

$$
\beta_c^U = \frac{\mu}{\Lambda_{\max}(H)},
\tag{17}
$$

where the elements of matrix H are $h_{ij} = \{1-(1-\gamma)f_i^{X\to Y}p_i^A\}[b_{ji} + (\iota-1)y_{ji}]$, $p_i^A = p_i^A(1-\delta) + p_i^U(1-r_i)$, and $\Lambda_{\max}(H)$ is the largest eigenvalue of H.

4.2. Numerical Simulations

To validate the threshold of epidemic outbreaks, we then explore the impacts of several key parameters (including the attenuation factor γ, the inter-layer feedback parameter τ and the mean group sizes $\bar{x}$, $\bar{y}$) on the propagation threshold. At first, we test how the attenuation factor γ and the inter-layer feedback parameter τ affect the threshold β_c in Figure 6.

As presented in Figure 6a, the threshold β_c is negatively correlated with the attenuation factor γ. According to the transmission mechanism, the physical layer nodes that have been alerted are infected by the low probability. However, with the increase of attenuation factor γ, the inhibitory level relatively becomes weak and then the epidemic is easy to spread, so the propagation threshold is reduced. According to Equation (2), the feedback intensity $f^{X\to Y}$ is enhanced with the increase of τ, so as to better restrain the epidemic spreading. As shown in Figure 6b, the threshold β_c is enhanced with the increasing feedback parameter τ. Moreover, from Figure 6, we notice that the large recovery probability μ and the small forgetting probability δ also help to inhibit epidemic spreading.
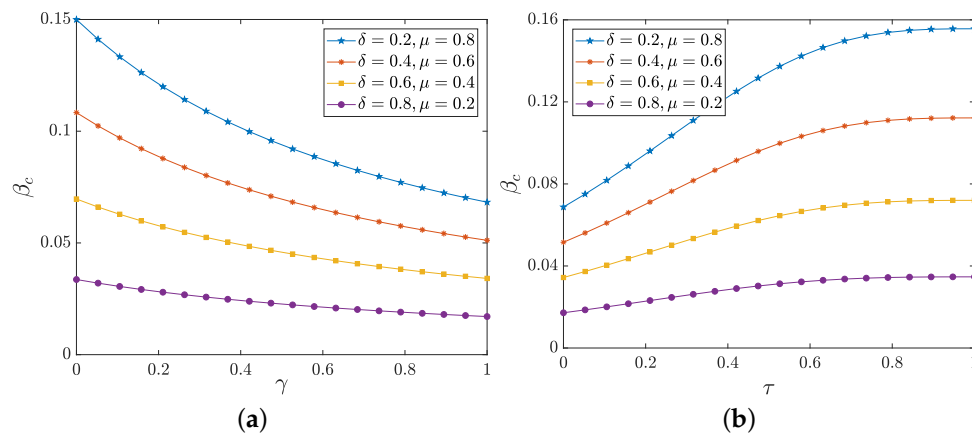
Figure 6. (**a**) The outbreak threshold β_c as a function of the attenuation factor γ. (**b**) β_c as a function of the inter-layer feedback parameter τ. The result of (**a**) is obtained for $\tau = 0.5$ and that of (**b**) is for $\gamma = 0.1$. Other parameters are fixed as $\lambda_1 = 0.9$, $\lambda_2 = 0.5$, $\iota = 1.1$, $\bar{x} = \bar{y} = 3$.

Next, in Figure 7, we show how the mean group sizes of information layer ($\bar{x}$) and physical layer ($\bar{y}$) take effects on the threshold of epidemic outbreaks β_c, respectively.
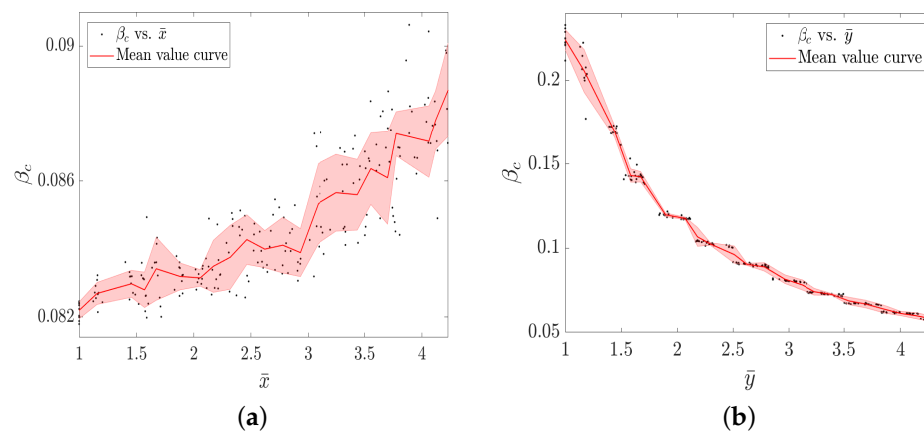
Figure 7. The epidemic spreading threshold β_c as functions of $\bar{x}$ (**a**) and $\bar{y}$ (**b**), respectively. Other parameters are: $\gamma = 0.1$, $\mu = \eta = \lambda_1 = 0.9$, , $\lambda_2 = \tau = 0.5$, $\iota = 1.1$, and $\bar{y} = 3$ ($\bar{x} = 3$) when studying how the $\bar{x}$ ($\bar{y}$) works on the β_c.

From Figure 7a, we observe that the increasing group sizes of the information layer $\bar{x}$ help to raise the threshold of epidemic outbreaks β_c, i.e., to inhibit the epidemic spreading. However, Figure 7b illustrates that the growth of the group size of the physical layer $\bar{y}$ reduces β_c. We thus take the conclusive results that the group growth of the information layer can better suppress the epidemic spreading while the group growth of the physical layer can promote the epidemic spreading. Therefore, the presented model and its findings verify the propagation principle in a general multilayer network with focus on the practical significance. Meanwhile, the findings consistent with common intuition demonstrate the feasibility and rationality of the proposed model. Hence, the existence of the group structure has a significant impact on the evolution of propagation processes on multilayer networks.

5. Network Propagation Robustness

In real life, the epidemic or information spreading process inevitably suffers from immunization measures or information islands and quarantine [38–40]. Meanwhile, many approaches use percolation theory to assess network robustness and prevent the spread of epidemics [41–44]. Based on

percolation theory, we then explore the propagation phenomena by considering two scenarios: disease immunization and occluded information dissemination. Disease immunization indicates that the immunized nodes will not be infected by the disease or spread to others, and occluded information dissemination means that the isolated nodes will not perceive the epidemic information or diffuse it. So these nodes which fail to engage in either epidemic or information propagation have no contribution to the coupled system, and then we can ignore the impact of the node on the whole propagation dynamics. We therefore consider attacking a proportion p_a ($0 \leq p_a \leq 1$) of nodes in both physical and information layers to simulate these two cases. Based on the foregoing analysis and conclusions, the group characteristic which changes the network connectivity have great influences on the propagation process. In this section, we aim to investigate how the information or physical connectivity variation (i.e., immunization or separation measure) further make influences on the coupled propagation dynamics and thus determine which connectivity structures have a more prominent role on the group-based multilayer network dynamics.

5.1. Disease Immunization

First, we evaluate the network propagation robustness in terms of the infected density ρ and the threshold of epidemic outbreak β_c by attacking a proportion p_a of physical layer nodes. Such action can be regarded as node immunization in some sense. Here four attack strategies are adopted, namely random attacks and three deliberate attacks based on degree centrality [45], closeness centrality [46] and eigenvector centrality [47]. Random attacks mean random deletion of nodes. Degree centrality attacks preferentially delete the nodes with large degrees. The nodes with a high closeness centrality are deleted with priority in the closeness centrality strategy. For the eigenvector centrality strategy, the nodes with high eigenvector centrality are preferentially attacked. As a comparison, we detect the propagation robustness of both the group-based multilayer network and the multiplex network, as shown in Figure 8.
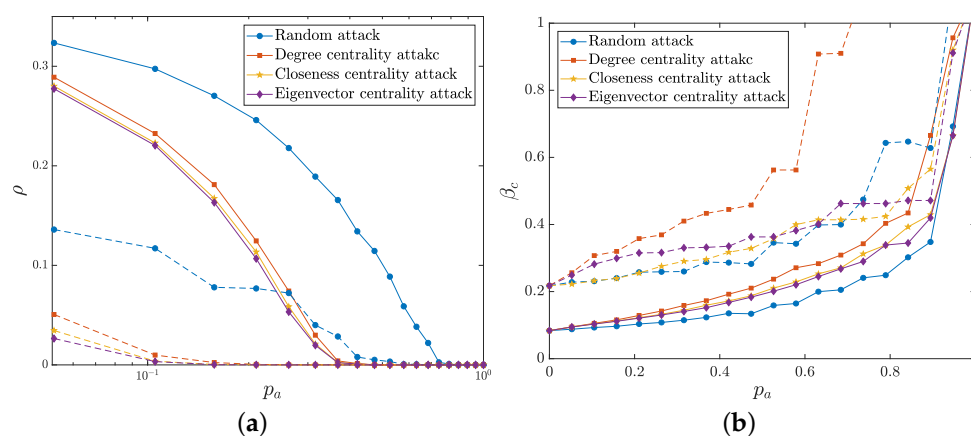

Figure 8. The I-state density ρ (**a**) and the epidemic threshold β_c (**b**) as functions of the attacked node proportion p_a under four attack strategies. The solid and dashed lines represent the variation of the group-based multilayer network and the multiplex network, respectively, where the lines in the same color indicate the same attack strategy. Other parameters are fixed as $\gamma = 0.1$, $\lambda_1 = \eta = \mu = 0.9$, $\beta = \tau = \delta = \lambda_2 = 0.5$, $\iota = 1.1$, and $\bar{x} = \bar{y} = 3$.

As shown in Figure 8a, the I-state density ρ of both the group-based multilayer network and the multiplex network declines with the increasing proportion of attacked nodes, which means that the isolation (i.e., immunization) of the nodes inhibits the epidemic spreading. We notice that the network propagation process is more robust to random attack than to deliberate attacks. Specifically, the density ρ of the group-based network is much higher than that of the multiplex network and is relatively slower to reach the $\rho = 0$ state. This phenomenon means that the propagation capacity and the robustness

of group-based multilayer network are better than those of the network without group structures. The variation of the threshold β_c in Figure 8b shows that β_c increases with the increase of deleted nodes of the physical layer. The epidemic outbreak is more sensitive to these deliberate attacks than to random attack. This finding suggests that targeted immunization may have more positive effects on the inhibition of epidemic outbreak. Moreover, the threshold of group-based multilayer network is smaller than that of multiplex network, thereby implying the group-based network is prone to epidemic outbreaks as a comparison with the multiplex network. Furthermore, the epidemic propagation threshold β_c changes gradually until most nodes are attacked (i.e., immunized). As a consequence, the simulated results illustrate that wide epidemic immunization appears to be quite necessary to efficiently control or even eliminate the epidemic outbreak.

5.2. Occluded Information Diffusion

Analogously, we study the propagation robustness of information layer as well as the variation of epidemic spreading by attacking their nodes. The infection density ρ and the epidemic threshold β_c versus the attacked proportion p_a are shown in Figure 9.
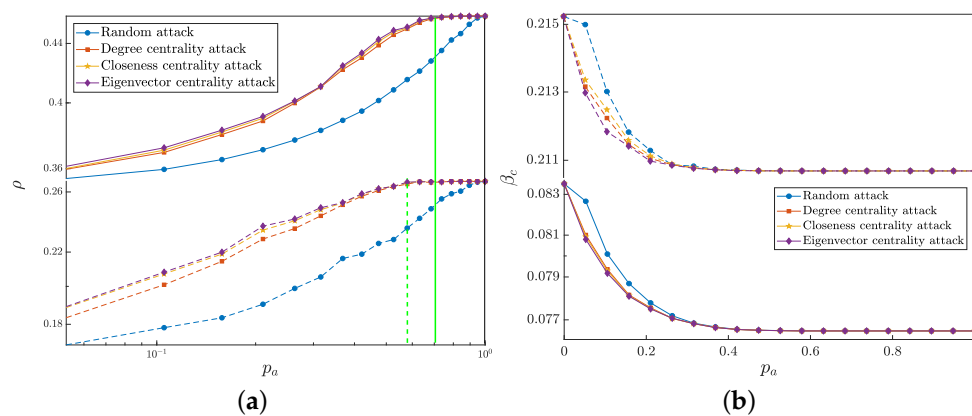

Figure 9. The I-state density ρ (**a**) and the threshold β_c (**b**) with respective to the attacked node proportion p_a under four attack strategies. The solid and dashed lines represent the variation of the group-based multilayer network and the multiplex network, respectively, where the lines in the same color represent the same attack strategy. Other parameters are fixed as $\gamma = 0.1$, $\lambda_1 = \eta = \mu = 0.9$, $\beta = \tau = \delta = \lambda_2 = 0.5$, $\iota = 1.1$, and $\bar{x} = \bar{y} = 3$.

From Figure 9, we find that the I-state density ρ increases with the attack proportion p_a while the threshold β_c decreases, which means that the occluded information dissemination enhances the epidemic spreading. In contrast to the disease immunity, the influence in this situation might be more mild due to the fact that attacking information layer nodes indirectly promotes epidemic spreading by inhibiting information diffusion. In Figure 9a, the green solid and dashed lines describe the attacked fraction when the infection density of the group-based multilayer network and the multiplex network reach their steady states, respectively. It is obvious that the networks with group structure need to attack more nodes when reaching its steady state than the networks without group structure, implying that the robustness of the group-based multilayer network is stronger than the multiplex network. In Figure 9b, we notice that random attack has the least impact on the propagation threshold β_c compared with deliberate attacks. Moreover, the threshold β_c from the group-based multilayer network is much lower than that from the multiplex network, which means that the propagation capacity of the group-based multilayer network is greater than the multiplex network.

6. Conclusions

In this paper, based on the proposed group-based bilayer network framework, we investigate the epidemic spreading in the physical layer which is affected by the information diffusion in the information layer. By employing MMCA to generate the probability transition trees to reveal the interplay between information diffusion and epidemic spreading, we find the group structure has a significant impact on the dynamics of disease transmission in the network. Specifically, the increase in the group size of the information layer inhibits the epidemic spreading and the increase in the group size of the physical layer promotes the epidemic spreading, which are manifested by the I-state density and the propagation threshold.

It is demonstrated that the capacity of epidemic spreading is negatively correlated with the inhibition of the information layer. Finally, we also considered the introduction of epidemic immunization and information diffusion suppression into the previous coupled propagation process, and then investigate the robustness of network propagation based on typical attack strategies. We conclude that such propagation is more vulnerable to deliberate attacks than to random attacks in terms of the I-state density and the threshold of the epidemic outbreak. Specifically, the propagation capacity and robustness of the group-based network are stronger than the multiplex network.

In summary, we explore a coupled propagation mechanism of a generally group-based multilayer network with focusing on the effects of the group structure and the inter-layer feedback mechanism on the spreading dynamics. Moreover, two scenarios (i.e., disease immunization and occluded information diffusion) are introduced to investigate the propagation robustness, which would help to give effective strategies to control epidemics.

References

1. Pastor-Satorras, R.; Vespignani, A. Epidemic spreading in scale-free networks. *Phys. Rev. Lett.* **2001**, *86*, 3200–3203. [CrossRef]
2. Pastor-Satorras, R.; Castellano, C.; Van Mieghem, P.; Vespignani, A. Epidemic processes in complex networks. *Rev. Mod. Phys.* **2015**, *87*, 925–979. [CrossRef]
3. Balcan, D.; Vespignani, A. Phase transitions in contagion processes mediated by recurrent mobility patterns. *Nat. Phys.* **2011**, *7*, 581–586. [CrossRef]
4. Vespignani, A. Modelling dynamical processes in complex socio-technical systems. *Nat. Phys.* **2011**, *8*, 32–39. [CrossRef]
5. Li, X.; Wang, X.F. Controlling the spreading in small-world evolving networks: Stability, oscillation, and topology. *IEEE Trans. Autom. Control* **2006**, *51*, 534–540. [CrossRef]
6. Saumellmendiola, A.; Serrano, M.A.; Boguna, M. Epidemic spreading on interconnected networks. *Phys. Rev. E* **2012**, *86*, 026106. [CrossRef]
7. Benczik, I.J.; Benczik, S.Z.; Schmittmann, B.; Zia, R.K. Opinion dynamics on an adaptive random network. *Phys. Rev. E* **2009**, *79*, 046104. [CrossRef]
8. Zhang, Z.K.; Liu, C.; Zhan, X.X.; Lu, X.; Zhang, C.X.; Zhang, Y.C. Dynamics of information diffusion and its applications on complex networks. *Phys. Rep.* **2016**, *651*, 1–34. [CrossRef]
9. Moreno, Y.; Nekovee, M.; Pacheco, A.F. Dynamics of rumor spreading in complex networks. *Phys. Rev. E* **2004**, *69*, 066130. [CrossRef]

10. Chierichetti, F.; Lattanzi, S.; Panconesi, A. Rumor spreading in social networks. *Theor. Comput. Sci.* **2011**, *412*, 2602–2610. [CrossRef]

11. Dolfin, M.; Knopoff, D.; Limosani, M.; Xibilia, M.G. Credit risk contagion and systemic risk on networks. *Mathematics* **2019**, *7*, 713. [CrossRef]

12. Hethcote, H.W. The mathematics of infectious diseases. *SIAM Rev.* **2000**, *42*, 599–653. [CrossRef]

13. Kurant, M.; Thiran, P. Layered Complex Networks. *Phys. Rev. Lett.* **2006**, *96*, 138701. [CrossRef]

14. Mucha, P.J.; Richardson, T.; Macon, K.; Porter, M.A.; Onnela, J.P. Community Structure in Time-Dependent, Multiscale, and Multiplex Networks. *Science* **2010**, *328*, 876–878. [CrossRef] [PubMed]

15. De Domenico, M.; Solé-Ribalta, A.; Cozzo, E.; Kivelä, M.; Moreno, Y.; Porter, M.A.; Gómez, S.; Arenas, A. Mathematical Formulation of Multilayer Networks. *Phys. Rev. X* **2013**, *3*, 041022. [CrossRef]

16. de Arruda, G.F.; Rodrigues, F.A.; Moreno, Y. Fundamentals of spreading processes in single and multilayer complex networks. *Phys. Rep.* **2018**, *756*, 1–59. [CrossRef]

17. De Domenico, M.; Granell, C.; Porter, M.A.; Arenas, A. The physics of spreading processes in multilayer networks. *Nat. Phys.* **2016**, *12*, 901–906. [CrossRef]

18. Granell, C.; Gómez, S.; Arenas, A. Dynamical interplay between awareness and epidemic spreading in multiplex networks. *Phys. Rev. Lett.* **2013**, *111*, 128701. [CrossRef]

19. Granell, C.; Gómez, S.; Arenas, A. Competing spreading processes on multiplex networks: Awareness and epidemics. *Phys. Rev. E* **2014**, *90*, 012808. [CrossRef]

20. Gómez, S.; Arenas, A.; Borge-Holthoefer, J.; Meloni, S.; Moreno, Y. Discrete-time Markov chain approach to contact-based disease spreading in complex networks. *EPL Eur. Lett* **2010**, *89*, 38009. [CrossRef]

21. Nie, X.Y.; Tang, M.; Zou, Y.; Guan, S.G.; Zhou, J. The impact of heterogeneous response on coupled spreading dynamics in multiplex networks. *Phys. A Stat. Mech. Its Appl.* **2017**, *484*, 225–232. [CrossRef]

22. Guo, Q.T.; Lei, Y.J.; Xia, C.Y.; Guo, L.; Jiang, X.; Zheng, Z.M. The Role of Node Heterogeneity in the Coupled Spreading of Epidemics and Awareness. *PLoS ONE* **2016**, *11*, e0161037. [CrossRef]

23. Gao, C.; Tang, S.T.; Li, W.H.; Yang, Y.Q.; Zheng, Z.M. Dynamical processes and epidemic threshold on nonlinear coupled multiplex networks. *Phys. A Stat. Mech. Its Appl.* **2018**, *496*, 330–338. [CrossRef]

24. Jiang, J.; Zhou, T. Resource control of epidemic spreading through a multilayer network. *Sci. Rep.* **2018**, *8*, 1629. [CrossRef]

25. Zang, H.J. The effects of global awareness on the spreading of epidemics in multiplex networks. *Phys. A Stat. Mech. Its Appl.* **2018**, *492*, 1495–1506. [CrossRef]

26. Guo, Q.T.; Jiang, X.; Lei, Y.J.; Li, M.; Ma, Y.F.; Zheng, Z.M. Two-stage effects of awareness cascade on epidemic spreading in multiplex networks. *Phys. Rev. E* **2015**, *91*, 012822. [CrossRef]

27. Sagar, V.; Zhao, Y. Collective effect of personal behavior induced preventive measures and differential rate of transmission on spread of epidemics. *Chaos* **2017**, *27*, 023115. [CrossRef]

28. Sagar, V.; Zhao, Y.; Sen, A. Effect of time varying transmission rates on the coupled dynamics of epidemic and awareness over a multiplex network. *Chaos* **2018**, *28*, 113125. [CrossRef]

29. Chen, X.L.; Wang, W.; Cai, S.M.; Stanley, H.E.; Braunstein, L.A. Optimal resource diffusion for suppressing disease spreading in multiplex networks. *J. Stat. Mech. Theory Exp.* **2018**, *2018*, 013007. [CrossRef]

30. Chen, X.L.; Wang, R.J.; Tang, M.; Cai, S.M.; Stanley, H.E.; Braunstein, L.A. Suppressing epidemic spreading in multiplex networks with social-support. *New J. Phys.* **2018**, *20*, 053501. [CrossRef]

31. Zheng, C.Y.; Xia, C.Y.; Guo, Q.T.; Dehmer, M. Interplay between SIR-based disease spreading and awareness diffusion on multiplex networks. *J. Parallel Distrib. Comput.* **2018**, *115*, 20–28. [CrossRef]

32. Xia, C.Y.; Wang, Z.S.; Zheng, C.Y.; Guo, Q.T.; Shi, Y.T.; Dehmer, M.; Chen, Z.Q. A new coupled disease-awareness spreading model with mass media on multiplex networks. *Inf. Sci.* **2019**, *471*, 185–200. [CrossRef]

33. Cozzo, E.; de Arruda, G.F.; Rodrigues, F.A.; Moreno, Y.; *Multiplex Networks: Basic Formalism and Structural Properties*, 1st ed.; Springer: Cham, Switzerland, 2018.

34. Szell, M.; Lambiotte, R.; Thurner, S. Multirelational organization of large-scale social networks in an online world. *Proc. Natl. Acad. Sci. USA* **2010**, *107*, 13636–13641. [CrossRef]

35. Battiston, S.; Caldarelli, C.; Garas, A.; *Multiplex and multilevel networks*, 1st ed.; Oxford University Press: Oxford, UK, 2019.

36. Bianconi, G. *Multilayer Networks: Structure and Function*, 1st ed.; Oxford University Press: Oxford, UK, 2018.

37. Erdös, P.; Rényi, A. On the Evolution of Random Graphs. *Bull. Int. Stat. Inst.* **1960**, *38*, 343–347.

38. Charkhgard, H.; Subramanian, V.; Silva, W.; Das, T.K. An integer linear programming formulation for removing nodes in a network to minimize the spread of influenza virus infections. *Discret. Optim.* **2018**, *30*, 144–167. [CrossRef]

39. Matamalas, J.T.; Arenas, A.; Gómez, S. Effective approach to epidemic containment using link equations in complex networks. *Sci. Adv.* **2018**, *4*. [CrossRef] [PubMed]

40. Zhou, M.Y.; Xiong, W.M.; Liao, H.; Wang, T.; Wei, Z.W.; Fu, Z.Q. Analytical connection between thresholds and immunization strategies of SIS model in random networks. *Chaos* **2018**, *28*, 051101. [CrossRef]

41. Liu, Y.Y.; Csóka, E.; Zhou, H.; Pósfai, M. Core Percolation on Complex Networks. *Phys. Rev. Lett.* **2012**, *109*, 205703. [CrossRef]

42. Huang, X.; Gao, J.; Buldyrev, S.V.; Havlin, S.; Stanley, H.E. Robustness of interdependent networks under targeted attack. *Phys. Rev. E* **2011**, *83*, 065101. [CrossRef]

43. Callaway, D.S.; Newman, M.E.J.; Strogatz, S.H.; Watts, D.J. Network Robustness and Fragility: Percolation on Random Graphs. *Phys. Rev. Lett.* **2000**, *85*, 5468–5471. [CrossRef]

44. Gallos, L.K.; Cohen, R.; Argyrakis, P.; Bunde, A.; Havlin, S. Stability and Topology of Scale-Free Networks under Attack and Defense Strategies. *Phys. Rev. Lett.* **2005**, *94*, 188701. [CrossRef]

45. Krackhardt, D. Assessing the Political Landscape—Structure, Cognition, and Power in Organizations. *Adm. Sci. Q.* **1990**, *35*, 342–369. [CrossRef]

46. Hage, P.; Harary, F. Eccentricity and Centrality in Networks. *Soc. Netw.* **1995**, *17*, 57–63. [CrossRef]

47. Brin, S.; Page, L. The anatomy of a large-scale hypertextual Web search engine. *Comput. Netw. ISDN Syst.* **1998**, *30*, 107–117. [CrossRef]